

# Solvability of The Output Corridor Control Problem by Pulse-Modulated Feedback <sup>★</sup>

Alexander Medvedev <sup>\*</sup> Anton V. Proskurnikov <sup>\*\*</sup>

<sup>\*</sup> Department of Information Technology, Uppsala University, SE-752 37 Uppsala, Sweden (e-mail: alexander.medvedev@it.uu.se)

<sup>\*\*</sup> Department of Electronics and Telecommunications, Politecnico di Torino, Turin, Italy, 10129 (e-mail: anton.p.1982@ieee.org).

**Abstract:** The problem of maintaining the output of a positive time-invariant single-input single-output system within a predefined corridor of values is treated. For third-order plants possessing a certain structure, it is proven that the problem is always solvable under stationary conditions by means of pulse-modulated feedback. The obtained result is utilized to assess the feasibility of patient-specific pharmacokinetic-pharmacodynamic models with respect to patient safety. A population of Wiener models capturing the dynamics of a neuromuscular blockade agent is studied to investigate whether or not they can be driven into the desired output corridor by clinically acceptable sequential drug doses (boluses). It is demonstrated that low values of a parameter in the nonlinear pharmacodynamic part lie behind the detected model infeasibility.

## 1. INTRODUCTION

Classical digital control addresses the problem of capturing essential continuous plant dynamics through the choice of the sampling time, often making use of engineering rules of thumb (Åström and Wittenmark, 2013). Then, the controller design is carried out utilizing the discretized model. Combined with model-based control algorithms, the necessity of high sampling rates resulted in significant computational burden, posing an implementation challenge to the control hardware of that time. Taking into account the inter-sample behavior in controller design emerged as an effective way of reducing the sampling rate to a minimum, an approach supported by sampled-data control theory (Tadmor, 1992).

The advances in the performance of control computers made the computation cheap and exceedingly high sampling rates readily available, thus rendering the sampled-data control tools inopportune. The transition from centralized to networked control highlighted the issues related to irregular sampling that stem from network imperfections, e.g., delays, packet loss, and jitter. These problems can be properly addressed by allowing irregular sampling in the framework of event-based control (Åström, 2008). Depending on the application, event-based control can reduce sampling rates by orders of magnitude, achieving similar performance to that of periodic sampling, while saving bandwidth and computation.

Asynchronous sampling of event-based control is still aimed at approximating the performance of regular discrete controllers, although with lower communication demand. Some control applications do not require tight feedback and allow for episodic adjustments of the control signal. A typical example of such an application is dosing,

that is, the process of administering a measured amount of a substance, which is often performed in a discrete manner.

A commonplace example of discrete dosing is following a doctor's orders on a medication regimen. Drug dosing often constitutes a repetitive and periodic activity where the doses and inter-dose intervals are adjusted to achieve the desired result and minimize the medication side effects. Interpreting administration of individual doses as impulsive action and allowing for measurement of the therapeutic effect directly leads to the concept of pulse-modulated feedback (Gelig and Churilov, 1998), where doses are manipulated through amplitude modulation and inter-dose intervals through frequency modulation. Yet, impulsive (or pulse-modulated) control is seldom used in the practice of drug dosing. Instead, standard process control techniques exploiting PID controllers and model-predictive controllers (MPC) dominate the area.

MPC is also possible in impulsive drug dosing setups. An application of impulsive MPC to control the intravenous bolus administration of lithium is reported in Sopasakis et al. (2015). A promising application of impulsive MPC is insulin dosing in simulated diabetes patients (Rivadeneira et al., 2020; Estremera et al., 2023). Impulsive control, even when applied to linear systems, introduces strongly nonlinear dynamics and, consequently, poses significant challenges in stability and robustness analysis. The introduction of online optimization complicates the situation.

A simple pulse-modulated controller that mimics pulsatile endocrine regulation and is suitable for discrete dosing applications has been suggested in Medvedev et al. (2024). Further study of the closed-loop dynamics arising when the controller is employed for the dosing of a neuromuscular blockade agent revealed complex nonlinear phenomena such as periodic solutions of high multiplicity, bistability, and deterministic chaos (Medvedev et al., 2025b). Bifurcation analysis is proposed as a way of avoiding undesired behaviors. Of course, it requires accurate patient-specific

<sup>★</sup> AM was partially supported by the Swedish Research Council under grant 2024-04943.

modeling of the pharmacokinetics and pharmacodynamics (PKPD), which is difficult to obtain from clinical data.

The contribution of this paper is twofold: First, it is proven that, for a certain class of third-order models, the problem of keeping the stationary plant output within a predefined corridor of values is always solvable by means of pulse-modulated feedback. Second, based on the obtained controller design insights, a method for assessing the feasibility of patient-specific PKPD models with respect to patient safety is proposed and illustrated on a previously published cohort (da Silva et al., 2012) of patient-specific models estimated from clinical data.

The rest of the paper is organized as follows. Section 2 defines the mathematical model at hand and formulates the output corridor impulsive control problem. Section 3 provides background information on necessary mathematical tools and previously proven results. Section 4 presents the main result of the paper; a sketch of the proof is given in the final Section 6. Section 5 describes the application to feasibility assessment of patient-specific PKPD models.

## 2. PROBLEM DEFINITION

We consider a continuous-time LTI system

$$\dot{x}(t) = Ax(t) + Bu(t), \quad y(t) = Cx(t), \quad (1)$$

driven by a train of impulses,

$$u(t) = \sum_{n=0}^{\infty} \lambda_n \delta(t - t_n), \quad 0 = t_0 < t_1 < t_2 < \dots \quad (2)$$

The system matrices have the following structure:

$$A = \begin{bmatrix} -a_1 & 0 & 0 \\ g_1 & -a_2 & 0 \\ 0 & g_2 & -a_3 \end{bmatrix}, \quad B = \begin{bmatrix} 1 \\ 0 \\ 0 \end{bmatrix}, \quad C = [0 \ 0 \ 1], \quad (3)$$

with distinct  $a_1, a_2, a_3 > 0$  and  $g_1, g_2 > 0$ . Since the matrix  $A$  is Metzler, system (1) is positive, that is,  $x(t) > 0$  for all  $t \in [0, \infty)$  whenever  $x(0) > 0$  and  $\lambda_n \geq 0$ .

Mathematically, system (1) under control law (2) is defined as a hybrid system, which evolves according to a continuous flow between the consecutive impulses,

$$\dot{x}(t) = Ax(t), \quad y(t) = Cx(t), \quad \forall t \in (t_n, t_{n+1}), \quad (4)$$

and undergoes instantaneous jumps in the state vector when an impulse occurs<sup>1</sup>:

$$x(t_n^+) = x(t_n^-) + \lambda_n B, \quad n = 0, 1, \dots \quad (5)$$

Feedback is enforced by modulating jump timing and magnitude with the continuous output,

$$T_n = \Phi(y(t_n)), \quad \lambda_n = F(y(t_n)), \quad t_{n+1} = t_n + T_n. \quad (6)$$

The design degrees of freedom of the pulse-modulated controller (6) are the frequency modulation function  $\Phi(\cdot)$  and the amplitude modulation function  $F(\cdot)$  that can be selected to achieve a variety of control objectives. To guarantee that the solutions are positive and bounded, it suffices to assume that these functions are bounded from above and below:

$$0 < \Phi_1 \leq \Phi(\cdot) \leq \Phi_2, \quad 0 < F_1 \leq F(\cdot) \leq F_2, \quad (7)$$

where  $\Phi_1, \Phi_2, F_1, F_2$  are constants.

In this paper, the following control problem is treated.

<sup>1</sup> The superscripts  $-$  and  $+$  in (5) denote the left-sided and right-sided limits, respectively.

**Output corridor impulsive control problem:** Given the plant (1), design the modulation functions  $\Phi(\cdot)$  and  $F(\cdot)$  of the impulsive feedback law (5), (6) to maintain the steady-state output  $y(t)$  in the corridor

$$y(t) \in [y_{\min}^*, y_{\max}^*], \quad y_{\min}^* > 0. \quad (8)$$

Since the solvability of this general problem is nontrivial, we study its modification: when does a special periodic solution termed a 1-cycle (see the definition in the next section) exist that satisfies (8)? This formally less general problem is important for two reasons: first, 1-cycles are the simplest periodic solutions of the hybrid system (one impulse over the least period); second, a design procedure exists that leads to a stable 1-cycle with predefined parameters (Medvedev et al., 2023a,b, 2024).

## 3. BACKGROUND

**Reduction to discrete-time dynamics:** It is easily seen that the trajectory of the hybrid closed-loop dynamics (4)-(6) is completely determined by the sequence  $X_n = x(t_n^-)$ , which evolves according to

$$X_{n+1} = e^{(t_{n+1} - t_n)A}(X_n + \lambda_n B), \quad n = 0, 1, \dots \quad (9)$$

where  $t_{n+1} - t_n$  and  $\lambda_n$  are determined by (6). Indeed, given  $X_n$ , the trajectory of (4) on the interval  $(t_n, t_{n+1})$  is

$$x(t) = e^{(t-t_n)A}(X_n + \lambda_n B), \quad t \in (t_n, t_{n+1}). \quad (10)$$

**1-cycles and their characteristics:** A periodic solution of (4)-(6) is called a 1-cycle if there is only one firing of the pulse-modulated feedback within the least period, i.e.,  $\lambda_n \equiv \lambda$ ,  $T_n \equiv T$  for all  $n = 0, 1, \dots$ . Then, a 1-cycle corresponds to a fixed point of the discrete map

$$X = Q(X), \quad Q(\xi) \triangleq e^{AT}(\xi + F(C\xi)B). \quad (11)$$

Assuming that  $F$  is nonincreasing and  $\Phi$  is nondecreasing (the hybrid system in this case turns into the impulsive Goodwin oscillator), the 1-cycle exists and is unique (Churilov et al., 2009; Proskurnikov et al., 2024).

For the problem in question, however, it is more important to design a 1-cycle with given parameters through the choice of appropriate modulation functions. It appears (Medvedev et al., 2023a) that the fixed point is uniquely determined by the 1-cycle parameters  $(\lambda, T)$ :

$$X = \lambda(e^{-AT} - I)^{-1}B. \quad (12)$$

Indeed, for a periodic solution to (4)-(6) with  $X_n \equiv X$ ,  $\lambda_n \equiv \lambda = F(CX)$ , and  $T_n \equiv T = \Phi(CX)$ , the relation (12) is obviously equivalent to  $X = Q(X)$ .

Notice that the expression (12) can be further simplified since the matrix exponential for the matrix  $A$  at hand is computed via the Opitz formula (De Boor, 2003, 2005). The first divided difference of a function  $\psi$  is defined as

$$\psi[\xi_0, \xi_1] \triangleq \frac{\psi(\xi_1) - \psi(\xi_0)}{\xi_1 - \xi_0},$$

where  $\xi_0 \neq \xi_1$ . The second divided difference is a function of three variables, defined by

$$\psi[\xi_0, \xi_1, \xi_2] \triangleq \frac{\psi[\xi_1, \xi_2] - \psi[\xi_0, \xi_1]}{\xi_2 - \xi_0},$$

where  $\xi_0, \xi_1, \xi_2$  are pairwise distinct.

*Proposition 1.* (Medvedev et al., 2023a, Proposition 2) The positive fixed point  $X = [X_1, X_2, X_3]^\top$  of the map  $Q$  in (11) is uniquely determined by the parameters of the 1-cycle:  $T > 0$  (the period) and  $\lambda > 0$  (the impulse weight). In terms of individual elements, it reads

$$\begin{aligned} X_1 &= \lambda\mu(-a_1T), \\ X_2 &= \lambda g_1 T \mu[-a_1 T, -a_2 T], \\ X_3 &= \lambda g_1 g_2 T^2 \mu[-a_1 T, -a_2 T, -a_3 T]. \end{aligned} \quad (13)$$

**The Output Corridor Problem for 1-Cycles:** We now focus on the following problem, stemming from the general output corridor control: find the parameters of the 1-cycle  $(\lambda, T)$  such that the output  $y(t) = Cx(t)$ , corresponding to the 1-cycle state  $x(t)$  from (9), (10), satisfies the corridor condition (8).

To handle this problem, we need the following extremal properties of the 1-cycle output  $y(t)$ . Notice that, for each  $0 \leq \tau \leq T$ , the output of the 1-cycle determined by the fixed point (12) is given by

$$y(\tau) = \lambda z(\tau), \quad z(\tau, T) \triangleq C e^{A\tau} (I - e^{AT})^{-1} B \quad (14)$$

due to (12). Using this representation, the following proposition can be proven (see Section 6).

*Proposition 2.* (Proskurnikov and Medvedev, 2025, Proposition 3) For every period  $T > 0$ , the equation

$$\frac{\partial z}{\partial \tau}(\tau, T) = C e^{A\tau} (I - e^{AT})^{-1} A B = 0 \quad (15)$$

has exactly two roots  $\tau_1$  and  $\tau_2$ , satisfying  $0 < \tau_1 < \tau_2 < T$ . These roots correspond, respectively, to the minimum and the maximum of the system output  $y(t)$ , defined by (14), on  $[0, T]$ . The output  $y(t)$  decreases on the intervals  $(0, \tau_1)$  and  $(\tau_2, T)$  and increases on  $(\tau_1, \tau_2)$ . The maximum and minimum of the output on  $[0, T]$  are, respectively,

$$y_{\max} = \lambda z(\tau_2, T) > X_3, \quad (16)$$

$$0 < y_{\min} = \lambda z(\tau_1, T) < X_3. \quad (17)$$

Due to the linearity of (5), the time instants  $\tau_1, \tau_2$  when the output  $y(t)$  achieves the extreme values are independent of  $\lambda$ , which, according to (12), scales the fixed point of the 1-cycle. Remarkably, the minimum of the output is achieved strictly between the impulses, which is counterintuitive since the jumps (5) increase the state vector. Nevertheless, the last coordinate  $y = x_3 = Cx$  is not directly affected by these jumps, and continues to decrease for some time  $\tau_1 > 0$  after the impulse.

## 4. MAIN RESULT

The main result of the paper is the positive answer to the problem from Section 3. Furthermore, for each range  $[y_{\min}^*, y_{\max}^*]$  there exist parameters  $(\lambda^*, T^*)$  such that the corridor constraint is tight for the 1-cycle corresponding to the fixed point  $X^*$ , that is,  $y_{\min} = y_{\min}^*$  and  $y_{\max} = y_{\max}^*$ .

For the function  $z$  introduced in (14), denote

$$z_{\max}(T) \triangleq z(\tau_2, T) = C e^{A\tau_2} (I - e^{AT})^{-1} B, \quad (18)$$

$$z_{\min}(T) \triangleq z(\tau_1, T) = C e^{A\tau_1} (I - e^{AT})^{-1} B. \quad (19)$$

Here  $\tau_1, \tau_2$  are the same as in Proposition 2.

*Theorem 3.* Given the output corridor (8) with  $0 < y_{\min}^* < y_{\max}^*$ , the equation

$$\Psi(T) \triangleq \frac{z_{\max}(T)}{z_{\max}(T) - z_{\min}(T)} = \frac{y_{\max}^*}{y_{\max}^* - y_{\min}^*} \quad (20)$$

always has a unique solution  $T^* > 0$ . Denoting

$$\lambda^* = \frac{y_{\max}^*}{z_{\max}(T^*)}, \quad (21)$$

the output of the 1-cycle with parameters  $(\lambda^*, T^*)$  satisfies (8); furthermore, both inequalities are tight:

$$y_{\min} = y_{\min}^*, \quad y_{\max} = y_{\max}^*.$$

The proof of Theorem 3 is given in Section 6. The key idea of the proof is illustrated by Fig. 1. The numerator of  $\Psi(T)$  (that is,  $z_{\max}(T)$ ) is a decreasing function with  $\lim_{T \rightarrow \infty} z_{\max}(T) = +\infty$ , while the denominator  $z_{\max} - z_{\min}$  is an increasing function on  $(0, \infty)$ . Also,  $z_{\max}(T)$  has a constant limit as  $T \rightarrow \infty$ , while  $z_{\min}(T)$  vanishes. Hence,  $\Psi(T) \rightarrow 1$  as  $T \rightarrow \infty$ ,  $\Psi(T) \rightarrow \infty$  as  $T \rightarrow 0$ , and  $\Psi$  is decreasing.

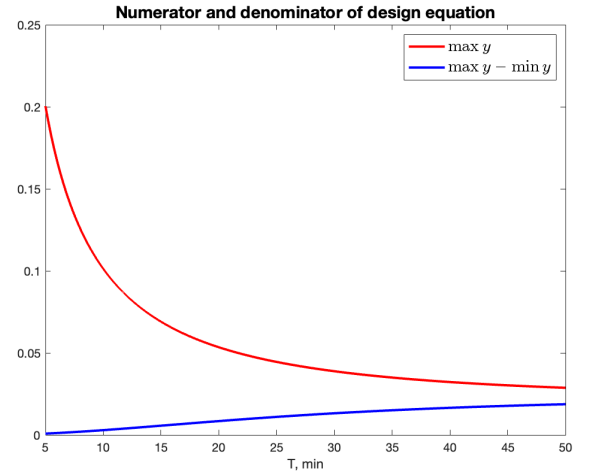


Fig. 1. Numerator and denominator of the function  $\Psi(T)$  in design equation (20). It can be seen that  $\lim_{T \rightarrow \infty} \Psi(T) = 1$ ,  $\lim_{T \rightarrow 0} \Psi(T) = \infty$

## 5. MODEL FEASIBILITY ANALYSIS

### 5.1 Model cohort

A minimal pharmacokinetic-pharmacodynamic (PKPD) Wiener model of the NMB agent *atracurium* is introduced in da Silva et al. (2012) and is intended for individualized control of drug delivery under general anesthesia.

The PK part of the model is given by the transfer function from the input  $u(t)$  to the serum drug concentration  $\bar{y}(t)$ :

$$W(s) = \frac{\bar{Y}(s)}{U(s)} = \frac{v_1 v_2 v_3 \alpha^3}{(s + v_1 \alpha)(s + v_2 \alpha)(s + v_3 \alpha)}. \quad (22)$$

Here,  $\bar{Y}(s) = \mathcal{L}\{\bar{y}(t)\}$ ,  $U(s) = \mathcal{L}\{u(t)\}$ , and  $\mathcal{L}\{\cdot\}$  denotes the Laplace transform. The parameters  $v_1 = 1$ ,  $v_2 = 4$ , and  $v_3 = 10$  are calculated from data at the population level and kept fixed across the cohort. The static gain of the transfer function (22) is normalized to one, and

$0 < \alpha \leq 0.1$  is the only patient-specific parameter. The PK model in (22) can be written in state-space form as

$$\dot{x}(t) = Ax(t), \quad \bar{y}(t) = Cx(t), \quad (23)$$

where the matrices are of the same structure as in (3), and  $a_1 = v_1\alpha$ ,  $a_2 = v_2\alpha$ ,  $a_3 = v_3\alpha$ ,  $g_1 = v_1\alpha$ ,  $g_2 = v_2v_3\alpha^2$ .

The PD part is modeled by a Hill function of order  $\gamma$ :

$$y = \varphi(\bar{y}) = \frac{100C_{50}^\gamma}{C_{50}^\gamma + \bar{y}^\gamma(t)}, \quad \gamma > 0, \quad (24)$$

where  $C_{50} = 3.2425 \mu\text{g ml}^{-1}$  is the drug concentration that yields 50% of the maximum effect. The output  $y(t)[\%]$  represents the effect of the NMB agent and is measured by a train-of-four (ToF) neuromuscular monitor, McGrath and Hunter (2006). The maximal level of  $y(t) = 100\%$  is achieved when the NMB is initiated and there is no drug in the patient's bloodstream.

With the model (22), (24), a patient's response to a drug dose is captured by a pair  $(\alpha, \gamma)$ . The dataset used in this study includes individualized models of 48 patients estimated from clinical data and is described in detail in da Silva et al. (2012). The model parameter estimates for the patient cohort are illustrated in Fig. 2. The population mean values amount to  $\bar{\alpha} = 0.0374$  and  $\bar{\gamma} = 2.6677$ .

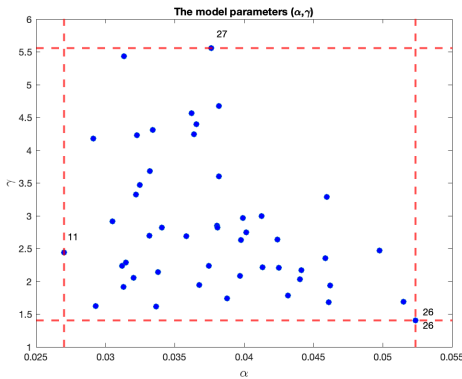


Fig. 2. The model parameter pairs in the dataset satisfy  $\alpha_{\min} = 0.0270 \leq \alpha \leq 0.0524 = \alpha_{\max}$ ,  $\gamma_{\min} = 1.4030 \leq \gamma \leq 5.5619 = \gamma_{\max}$ . The extreme parameter values are indicated by the Patient Identification Number (PIN). PIN 26 features two extreme values and corresponds to  $(\alpha_{\max}, \gamma_{\min})$ .

## 5.2 Feasibility analysis

When using *atracurium* in surgical practice, NMB is initiated with a bolus dose of 400–500  $\mu\text{g/kg}$ . Further into the procedure, maintenance doses of 80–200  $\mu\text{g/kg}$  are administered every 15–25 min. Dosing varies widely among patients and is individualized based on continuous monitoring of neuromuscular function, e.g., by a ToF monitor. According to (da Silva et al., 2012, Fig. 4), the NMB depth is to be kept within the range  $2\% \leq y(t) \leq 10\%$  throughout the surgery.

A practical way of evaluating the feasibility of the estimated models is to calculate what bolus doses and timing are required to maintain the model output within the prescribed corridor. This test is important to enforce patient

safety and exclude models whose use in impulsive feedback dosing would lead to violation of the recommended drug regimen. Indeed, with a patient-specific PKPD model expressed in terms of two constants (cf. (22), (24)) and without any apparent connection to the purpose of medication, the model feasibility is difficult to evaluate. The results of Proposition 2 and Theorem 3 support a straightforward procedure that allows one to judge whether or not a PKPD model estimated from data is suitable for the calculation of sequential bolus doses.

The model feasibility evaluation procedure is as follows.

**Step 1:** Set the output corridor limits in (8) to  $y_{\min}^* = 2$ ,  $y_{\max}^* = 10$ , according to the clinical recommendations.

**Step 2:** By inverting the PD function in (24), calculate  $\bar{y}_{\min}^* = \varphi^{-1}(y_{\min}^*)$ ,  $\bar{y}_{\max}^* = \varphi^{-1}(y_{\max}^*)$ .

**Step 3:** Given the matrices  $A, B, C$  of the patient-specific model, solve the design equation

$$\frac{z_{\max}(T)}{z_{\max}(T) - z_{\min}(T)} = \frac{\bar{y}_{\max}^*}{\bar{y}_{\max}^* - \bar{y}_{\min}^*}$$

and obtain the value of  $T^*$ .

**Step 4:** Calculate the bolus dose

$$\lambda^* = \frac{\bar{y}_{\max}^*}{z_{\max}(T^*)}.$$

**Step 5:** Check whether the pair  $(T^*, \lambda^*)$  (the dosing parameters) is within the clinically feasible range.

Calculations of  $(T^*, \lambda^*)$  for all patient models in the cohort have been performed according to the procedure above, and the results are summarized in Fig. 3. It is instructive to examine the locations of the dosing parameters for the patient models with the extreme values of  $\alpha$  and  $\gamma$ , i.e., PIN=11,26,27. Notably, the maximal value of  $\gamma$  does not present a challenge (PIN=27) when it comes to output corridor control. In contrast, low values of  $\alpha$  and  $\gamma$  demand either excessively high drug doses or very long intervals between the dosing instants, to satisfy (8). Within the considered cohort, there is no model that yields a combination of low  $\lambda^*$  and high  $T^*$ .

To clarify the patterns in the parameters  $(\alpha, \gamma)$  resulting in infeasible patient models, the scatter plot in Fig. 2 is repeated in Fig. 4, but with the parameter pairs corresponding to infeasible models highlighted by filled circles. A common property of all the infeasible models is low values of  $\gamma$ , i.e. the slope of the Hill function in (24). Apparently, a low value of  $\gamma$  makes the model infeasible regardless of the value of  $\alpha$ .

There are several possible explanations for why some of the identified Wiener PKPD models do not agree with clinical dosing practices. First of all, the mode of drug administration considered in the present paper, i.e., sequential boluses, is not the same as the one covered in the data underlying the PKPD modeling in da Silva et al. (2012) – the continuous infusion. By its sheer nature, impulsive control requires mathematical models that are accurate over a larger range of input amplitudes, whereas a controller stabilizing the closed-loop system in the vicinity of a stationary point can be obtained based on a model that approximates the plant dynamics at this particular point. Further, as pointed out in da Silva et al. (2012), the plant excitation is typically low in drug

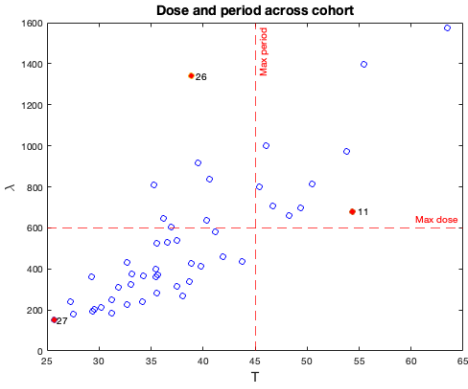


Fig. 3. Calculated values of  $\lambda^*$  and  $T^*$  across the cohort of patient models. The dashed lines show the highest clinically feasible values:  $\lambda_{\max} = 600 \mu\text{g/kg}$ ,  $T_{\max} = 45 \text{ min}$ . The cases exhibiting the extreme values of  $\alpha$  and  $\gamma$  (in red) are marked with PIN; cf. Fig. 2.

infusion applications, which inevitably leads to poor model parameter estimates, especially those related to the model nonlinearity.

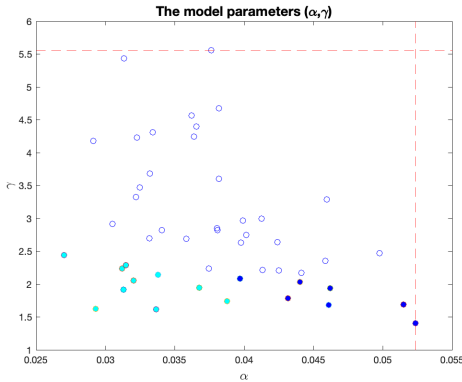


Fig. 4. The model parameter pairs  $(\alpha, \gamma)$  in the dataset. Infeasible models are marked with filled circles. Models with  $\lambda^* < \lambda_{\max}$  and  $T^* < T_{\max}$  are plotted in blue, and models with  $\lambda^* > \lambda_{\max}$  and  $T^* > T_{\max}$  are plotted in cyan.

## 6. PROOFS OF THE MAIN RESULTS

We start by establishing some properties of the functions  $\tau_1 = \tau_1(T)$  and  $\tau_2 = \tau_2(T)$  for  $T > 0$ ; the proof of Proposition 2 will also be given in the next subsection.

### 6.1 The Existence and Technical Properties of $\tau_1, \tau_2$

The next lemma follows from the general theory of  $T$ -systems (Chebyshev systems) (Karlin and Studden, 1966).

**Lemma 1.** Let  $\alpha_1, \dots, \alpha_n \in \mathbb{R}$  be pairwise distinct and let  $\sum_{i=1}^n |c_i| > 0$ , where  $c_1, \dots, c_n \in \mathbb{R}$ . Then the equation

$$\varrho(t) \triangleq \sum_{j=1}^n c_j e^{t\alpha_j} = 0$$

has no more than  $n - 1$  real solutions.

Lemma 1 entails the following property of the linear system (1), (3) impulse response.

**Proposition 4.** The impulse response  $g(t) = Ce^{tA}B$  of linear system (1), (3) attains its peak at some  $t_* \in (0, \infty)$ , increasing on  $[0, t_*]$  and decreasing on  $(t_*, \infty)$ .

**Proof.** System (1) has a nonzero transfer function from  $u$  to  $y$ ; hence  $g(t)$  and  $\dot{g}(t)$  are nonzero linear combinations of the modal functions  $e^{-\alpha_i t}$ . By Lemma 1,  $g$  has at most two stationary points where  $\dot{g} = 0$ . One of these stationary points is  $t = 0$ , because  $\dot{g}(0) = CAB = 0$  in view of (3). Since  $g(0) = CB = 0$  and  $g(t) \rightarrow 0$  as  $t \rightarrow \infty$ , the function  $g$  cannot be strictly increasing on  $(0, \infty)$ ; in other words,  $\dot{g}$  cannot be sign-preserving. Hence, another stationary point  $t_* \in (0, \infty)$  exists. By noticing that  $\ddot{g}(0) = CA^2B > 0$ , it follows that  $\dot{g}(t) > 0$  (i.e.,  $g(t)$  increases) for  $0 < t < t_*$  and  $\dot{g}(t) < 0$  (i.e.,  $g(t)$  decreases) for  $t > t_*$ . ■

Proposition 2 is proved similarly.

**Proof of Proposition 2** For  $T > 0$  being fixed, denote  $X_T := (e^{-TA} - I)^{-1}B$  and  $z(\tau) := z(\tau, T)$ . Then,  $z(T) = CX_T$ . Furthermore,  $z(0) = z(T)$ , since  $CB = 0$  and

$$z(0) - z(T) = C(I - e^{TA})(I - e^{TA})^{-1}B = CB = 0.$$

Similarly, using the relation  $CAB = 0$ , the derivative

$$\dot{z}(\tau) = C e^{\tau A} A(I - e^{\tau A})^{-1}B$$

satisfies the periodicity condition  $\dot{z}(0) = \dot{z}(T) = CAX_T < 0$ . The latter inequality holds, because  $AX_T$  is a negative vector (Medvedev et al., 2023a, Proposition 3). Therefore,  $z(0) = z(T)$  is neither the minimum nor the maximum value of  $z(\cdot)$  on the interval  $[0, T]$ . Since, by the Weierstrass theorem,  $z(\cdot)$  attains its minimum and maximum values on  $[0, T]$ , there exist at least two extremal points  $\tau_1, \tau_2$  with  $0 < \tau_1 < \tau_2 < T$  such that  $\dot{z}(\tau_i) = 0$ , or, equivalently,  $\tau = \tau_i$  is a solution of (15). According to Lemma 1, equation (15) cannot have more than two real roots since its left-hand side (for fixed  $T$ ) is a nonzero linear combination of  $e^{-\alpha_i \tau}$ ,  $i = 1, 2, 3$ . Hence,  $\tau_1$  and  $\tau_2$  are the only points where  $\dot{z}$  can change sign. Recalling that  $\dot{z}(0) = \dot{z}(T) < 0$ , it follows that  $\dot{z}$  is negative on  $(0, \tau_1)$  and  $(\tau_2, T)$ , and positive on  $(\tau_1, \tau_2)$ . Consequently,  $\tau_1$  is the point of minimum, and  $\tau_2$  is the point of maximum, which completes the proof of (16) and (17) since  $y(\tau) = \lambda z(\tau, T)$  for all  $\tau \in [0, T]$  and the fixed point is  $X = \lambda X_T$ . ■

Notice that, in accordance with Proposition 4, one has  $\dot{g}(t) = CA e^{tA} B < 0$  for  $t > t_*$ , in particular,

$$\frac{dz(\tau, T)}{d\tau} = CA e^{\tau A} (I - e^{TA})^{-1}B = \sum_{k=0}^{\infty} CA e^{(\tau+kT)A} B < 0$$

for any  $\tau \geq t_*$ . This entails the following corollary.

**Corollary 5.** For any  $T > 0$ , one has  $0 < \tau_1(T) < \tau_2(T) < t_*$ . Furthermore, the following limit relations hold:

$$\begin{aligned} \tau_1(T) &\xrightarrow{T \rightarrow \infty} 0, & \tau_2(T) &\xrightarrow{T \rightarrow \infty} t_*, \\ z_{\min}(T) &\xrightarrow{T \rightarrow \infty} 0, & z_{\max}(T) &\xrightarrow{T \rightarrow \infty} g(t_*). \end{aligned} \quad (25)$$

**Proof.** The first statement follows immediately from Propositions 4 and 2: recall that  $\dot{g}(t) \geq 0$  for  $t \in [\tau_1, \tau_2]$ , which means that  $[\tau_1, \tau_2] \cap [t_*, \infty) = \emptyset$ , i.e.,  $\tau_2(T) < t_*$  for all  $T$ . Hence, for  $T > t_*$ , the minimum and maximum of  $z(\tau, T)$  on the intervals  $[0, T]$  and  $[0, t_*]$  are identical.

The relations (25) now follow from the fact that  $z(\tau, T)$  converges to  $g(\tau)$  uniformly in  $\tau \in [0, t_*]$  as  $T \rightarrow \infty$ , i.e.,

$$\max_{0 \leq \tau \leq t_*} |z(\tau, T) - g(\tau)| \xrightarrow{T \rightarrow \infty} 0,$$

and from the fact that  $g(t)$  attains a unique global minimum (equal to 0, at  $t = 0$ ) and a unique global maximum (at  $t = t_*$ ) on  $[0, t_*]$ .

It can be easily shown that  $z_{\min}$  and  $z_{\max}$  tend to  $\infty$  as  $T \rightarrow 0$ , however,  $z_{\max} - z_{\min}$  remains bounded (in fact, simulations suggest that this function vanishes as  $T \rightarrow 0$ ; see Fig. 1). We formulate the following corollary.

**Corollary 6.** The following limit relations hold:

$$\begin{aligned} z_{\min}(T) &\xrightarrow{T \rightarrow 0} +\infty, & z_{\max}(T) &\xrightarrow{T \rightarrow 0} +\infty, \\ \limsup_{T \rightarrow 0} (z_{\max}(T) - z_{\min}(T)) &< \infty. \end{aligned} \quad (26)$$

**Proof.** Notice that  $(I - e^{TA})^{-1} = -\frac{1}{T}A^{-1} + O(1)$  as  $T \rightarrow 0$ . Since  $(-CA^{-1}B) = \frac{g_2g_1}{a_1a_2a_3} > 0$ , one has

$$z_{\max}(T) > z(0, T) = -\frac{1}{T}(CA^{-1}B) + O(1) \xrightarrow{T \rightarrow 0} \infty.$$

The mean value theorem guarantees that

$$0 < z(\tau_2, T) - z(\tau_1, T) = (\tau_2 - \tau_1) \frac{\partial}{\partial \tau} z(\tau, T) \Big|_{\tau=\xi},$$

where where  $0 < \tau_1 < \xi < \tau_2 < T$  (the point  $\xi = \xi(T)$  depends on  $T$ ). Since  $0 < \tau_2 - \tau_1 < T$  and, in view of (15), the derivative is  $O(1/T)$  as  $T \rightarrow 0$ , the right-hand side remains bounded as  $T \rightarrow 0$ . ■

Introduce the function

$$\hat{z}(\tau, T) = \begin{cases} z(\tau, T), & \tau \leq T, \\ z(T, T), & \tau > T. \end{cases}$$

It follows from Proposition 2 that  $\tau_1(T)$  and  $\tau_2(T)$  are the unique argmin and argmax, respectively, of  $\hat{z}(\cdot, T)$  on  $[0, \infty)$ . Since  $\hat{z}$  is continuous on  $[0, \infty) \times (0, \infty)$ , Berge's Maximum Theorem (Ok, 2007) yields the following.

**Corollary 7.** The functions  $\tau_1, \tau_2, z_{\min}, z_{\max}$  are continuous on  $(0, \infty)$ .

Applying Danskin's theorem Danskin (1967) to the function  $\hat{z}$ , which is  $C^\infty$ -smooth for  $\tau, T > 0$ , one can show that  $z_{\min}$  and  $z_{\max}$  are differentiable with respect to  $T$ , and their derivatives are continuous functions as follows

$$\dot{z}_{\min}(T) = \frac{\partial z}{\partial T} z(\tau_1(T), T) = CA e^{A(T+\tau_1)} (I - e^{AT})^{-2} B,$$

$$\dot{z}_{\max}(T) = \frac{\partial z}{\partial T} z(\tau_2(T), T) = CA e^{A(T+\tau_2)} (I - e^{AT})^{-2} B.$$

Using this representation, the following proposition can be proven, illustrated by Fig. 1.

**Proposition 8.** The functions  $z_{\min}, z_{\max}$  are decreasing on  $(0, \infty)$ , whereas their difference  $z_{\max} - z_{\min}$  is increasing.

**Proof.** Introduce the vector  $X_T := (e^{-TA} - I)^{-1}B$ . Then

$$\dot{z}_{\min}(T) = C e^{\tau_1 A} (I - e^{AT})^{-1} A X_T < 0,$$

since  $A X_T < 0$  Medvedev et al. (2023a) and

$$e^{\tau_1 A} (I - e^{AT})^{-1} = \sum_{k=0}^{\infty} e^{A(\tau_1 + kT)}$$

is a nonnegative matrix with positive row sums. Hence, the product  $e^{\tau_1 A} (I - e^{AT})^{-1} A X_T$  is a strictly negative vector; in particular, its last coordinate (selected by multiplication with  $C$ ) is negative.

For the same reason, one has  $\dot{z}_{\max}(T) < 0$  (in the previous argument,  $\tau_1$  can be replaced by  $\tau_2$ ).

Using the mean value theorem, one has

$$\dot{z}_{\max} - \dot{z}_{\min} = (\tau_2 - \tau_1) C A^2 e^{\theta T A} (I - e^{AT})^{-2} B,$$

where  $\tau_1(T) \leq \theta T \leq \tau_2(T) < 2T$ , and hence  $1 < \theta < 2$  (the point  $\theta$  depends on  $T$ ). Using the Opitz formula (Medvedev et al., 2023a, Appendix), one can show that the latter expression is positive since the function  $\rho_\theta(s) = s^2 e^{\theta s} (1 - e^s)^{-2}$  is convex on  $(-\infty, 0)$ , and hence  $C \rho_\theta(T A) B > 0$ . ■

## 6.2 Proof of Theorem 3

Since  $z_{\min}$  and  $z_{\max}$  are continuous (Corollary 7), the function  $\Psi(\cdot)$  in (20) is continuous. According to (25) and (26), its limits as  $T \rightarrow 0$  and  $T \rightarrow \infty$  are, respectively,  $\infty$  and 1. Hence, this function takes all values in the interval  $(1, \infty)$ , in particular, the equation (20) has a solution. Proposition 8 ensures that the function  $\Psi$  is monotone decreasing as  $z_{\max}$  is decreasing and  $z_{\max} - z_{\min}$  is increasing, hence, the solution is unique.

The remaining parts are straightforward from Proposition 2. ■

## CONCLUSIONS

The solvability of the output corridor impulsive control problem is investigated. It is proven that the output of a linear positive plant comprising a cascade of three first-order blocks can always be controlled to a pre-defined corridor of values by a pulse-modulated feedback. The obtained result is shown to be useful in feasibility analysis of identified minimal patient-specific pharmacokinetic-pharmacodynamic models. The algorithm for calculating the exact upper and lower bounds of the stationary periodic solution with one firing of the impulsive feedback on the least period (1-cycle) allows solving the converse problem. Then, for a desired output corridor and given plant model, the drug dose and inter-dose period can be calculated and compared to clinically practiced regimen.

## REFERENCES

- Åström, K.J. (2008). Event based control. In *Analysis and design of nonlinear control systems: In honor of Alberto Isidori*, 127–147. Springer.
- Åström, K.J. and Wittenmark, B. (2013). *Computer-controlled systems: theory and design*. Courier Corp.
- Churilov, A., Medvedev, A., and Shepeljavyi, A. (2009). Mathematical model of non-basal testosterone regulation in the male by pulse modulated feedback. *Automatica*, 45(1), 78–85.
- da Silva, M.M., Wigren, T., and Mendonca, T. (2012). Nonlinear identification of a minimal neuromuscular blockade model in anesthesia. *IEEE Transactions on Control Systems Technology*, 20(1), 181–188.
- Danskin, J.M. (1967). *The Theory of Max-Min and its Application to Weapons Allocation Problems*, volume 5 of *Econometrics and Operations Research*. Springer-Verlag, Berlin, Heidelberg.

De Boor, C. (2003). A Leibniz formula for multivariate divided differences. *SIAM Journal on Numerical Analysis*, 41(3).

De Boor, C. (2005). Divided differences. *Surveys in Approximation Theory*, 1, 46–69.

Estremera, E., Beneyto, A., Cabrera, A., Contreras, I., and Vehí, J. (2023). Intermittent closed-loop blood glucose control for people with type 1 diabetes on multiple daily injections. *Computer Methods and Programs in Biomedicine*, 236, 107568.

Gelig, A.K. and Churilov, A.N. (1998). *Stability and oscillations of nonlinear pulse-modulated systems*. Springer Science & Business Media.

Karlin, S. and Studden, W.J. (1966). *Tchebycheff Systems: With Applications in Analysis and Statistics*. Interscience Publishers, New York.

McGrath, C.D. and Hunter, J.M. (2006). Monitoring of neuromuscular block. *Continuing Education in Anaesthesia Critical Care & Pain*, 6(1), 7–12.

Medvedev, A., Proskurnikov, A.V., and Zhusubaliyev, Z.T. (2024). Output corridor control via design of impulsive Goodwin's oscillator. In *2024 American Control Conference (ACC)*, 5419–5424. IEEE.

Medvedev, A., Proskurnikov, A.V., and Zhusubaliyev, Z. (2023a). Design of the impulsive Goodwin's oscillator: A case study. In *Amer. Control Conf.*, 3572–3577.

Medvedev, A., Proskurnikov, A.V., and Zhusubaliyev, Z. (2023b). Design of the impulsive Goodwin's oscillator in 1-cycle. In *IFAC World Congress*. Yokohama, Japan.

Medvedev, A., Proskurnikov, A.V., and Zhusubaliyev, Z.T. (2025a). Design of cycles by impulsive feedback: Application to discrete dosing. *To be submitted, online on ArXiv*.

Medvedev, A., Proskurnikov, A.V., and Zhusubaliyev, Z.T. (2025b). Nonlinear dynamics in pulse-modulated feedback drug dosing. In *47th Annual International Conference of the IEEE Engineering in Medicine and Biology Society*. Copenhagen, Denmark.

Ok, E.A. (2007). *Real Analysis with Economic Applications*. Princeton University Press, Princeton, NJ.

Proskurnikov, A. and Medvedev, A. (2025). Output corridor control by pulse-modulated feedback. (*submitted*).

Proskurnikov, A.V., Runvik, H., and Medvedev, A. (2024). Cycles in impulsive Goodwin's oscillators of arbitrary order. *Automatica*, 159, 111379.

Rivadeneira, P.S., Godoy, J., Sereno, J., Abuin, P., Ferramosca, A., and González, A. (2020). Impulsive MPC schemes for biomedical processes: Application to type 1 diabetes. In A.T. Azar (ed.), *Control Applications for Biomedical Engineering Systems*, 55–87.

Sopasakis, P., Patrinos, P., Sarimveis, H., and Bemporad, A. (2015). Model predictive control for linear impulsive systems. *IEEE Transactions on Automatic Control*, 60(8), 2277–2282.

Tadmor, G. (1992).  $H^\infty$  optimal sampled-data control in continuous time systems. *International Journal of Control*, 56(1), 99–141.